

УДК 519.876.5, 551.510.535, 621.37

## Multidimensional Free Interpolation Framework for High-precision Modeling of Slant Total Electron Contents in Mid-latitude and Equatorial Regions

**Sergey P. Tsarev\***

Institute of Space and Information Technologies  
Siberian Federal University  
Svobodny 79, Krasnoyarsk, 660041  
Russia

**Valery V. Denisenko†**

Institute of Computational Modeling SB RAS  
Academgorodok 50, Krasnoyarsk, 660036  
Institute of Mathematics and Computer Science  
Siberian Federal University  
Svobodny 79, Krasnoyarsk, 660041  
Russia

**Marat M. Valikhanov‡**

Institute of Engineering Physics and Radioelectronics  
Siberian Federal University  
Svobodny 79, Krasnoyarsk, 660041  
Russia

---

Received 06.04.2018, received in revised form 06.07.2018, accepted 06.10.2018

*Standard models of ionospheric delays have errors of order 1–8 TECU (standard total electron content units). On the basis of the free interpolation framework we propose a new simple model of the slant TEC distributions approximating slant TEC distributions obtained from the three-dimensional ionospheric models NeQuick2 and IRI-2016 with RMS error < 0.05 TECU. The proposed model was tested for various positions of receivers in mid-latitude and equatorial regions. Stability of the coefficients of the model with respect to the position of the receiver and time is substantiated.*

*Keywords: ionosphere, total electron content, GLONASS, GPS, interpolation, machine learning.*

DOI: 10.17516/1997-1397-2018-11-6-781-791.

---

## Introduction

Ionospheric delays are an important factor in degradation of navigation precision for users of global navigation satellite systems (GNSS) so their modeling and mitigation is an active field of research. Neglecting higher-order effects (they usually do not exceed a few centimeters, [1]) one can reduce estimation of ionospheric delays to estimation of the so-called total electron content (TEC) along the straight lines connecting a receiver and GNSS satellites. The well-known models of ionospheric delays widely used in GNSS practice [2–7] have an accuracy of 1–8

---

\*sptsarev@mail.ru

†denisen@icm.krasn.ru

‡mvalihanov@sfu-kras.ru

© Siberian Federal University. All rights reserved

TECU (standard units of total electronic content) which is approximately equivalent to 0.15–1.2 meter in terms of pseudorange errors for GPS L1 frequency. These models are mainly based on the approximation of the real three-dimensional distribution of electrons in the ionosphere by a single-layer or two-layer distribution. Three-dimensional ionosphere models don't use this rough assumption but they are complicated and still have reduced precision due to modeling latency and difficulties in modeling of short-term mesoscale ionospheric disturbances and other complicated ionospheric phenomena. A typical distribution of electron concentration in the ionosphere given by the NeQuick2 model [8] is shown below on Fig. 1. It clearly shows why single-layer or even multi-layer ionospheric models have fundamental precision limitations.

We propose a new model of ionospheric delays, significantly more accurate than single and double layer approximations, but simple enough for practical use in radionavigation. It is based on the free interpolation framework, successfully applied in [10, 11] (under the name of “universal interpolation framework”) to the problem of high-precision reconstruction of GNSS satellite orbits using SP3 data. Our framework is not limited to polynomials, trigonometric or spherical functions conventionally used as the basis for interpolation. The interpolating basis in our framework automatically adapts to the data to be interpolated and uses a simple machine learning approach. Due to this simple trick the accuracy of our free interpolation framework (as we have demonstrated below and in [10, 11]) is much higher than the accuracy of the traditional models of ionospheric delays. Our framework still retains a relatively small number of parameters unlike the three-dimensional models.

In this paper we make a first step towards the modeling and determination of real slant TEC (STEC) values, namely we investigate the level of approximation of our model to widely used three-dimensional ionospheric models. Adequacy of our model for real-time determination of ionospheric delays and accompanying determination of differential code and phase biases (DCBs, cf. [4]) from dual-frequency receiver measurements as well as incorporation of higher-order ionospheric effects into the free interpolation framework will be studied later.

As shown below, our model of ionospheric delays is quite universal, stable over time and provides (with a relatively small number of parameters) the values of STEC having standard deviation  $< 0.05$  TECU from those calculated using the modern three-dimensional empirical models of the ionosphere. Thus our model, keeping expressions for STEC calculation simple (cf. (2)), has no fundamental precision limitations typical for the models based on layered electron density distributions.

## 1. Three-dimensional models of the ionosphere used for calculation of the slant TEC distributions

We used two empirical models of the space-time distribution of electron concentration: IRI-2016 [9], and NeQuick2 [8]. IRI-2016 gives the space distribution of the electron density  $N_e$  for heights from 65 km in the day-time and from 80 km in the night-time ionosphere to 2000 km. To calculate STEC, we integrate  $N_e$  along various inclined (“slant”) rays starting at the selected point on the surface of the Earth (receiver location), to the height of 2000 km. The NeQuick2 model gives the distribution of  $N_e$  from 90 km to 20,000 km and has its own functions for STEC calculation. Fig. 1 shows the meridional cross-section of the distribution of the electron concentration  $N_e$  in the model NeQuick2 for the Greenwich meridian for midnight UT, 03.22.2002, in conditions of equinox with high solar activity  $F10.7 = 160$ , Northern hemisphere. Bold curves are the lines of constant value of  $\log_{10} N_e$  with a contour interval  $1/3$ , where  $N_e$  is given in

$\text{m}^{-3}$  units. Dashed lines correspond to values less than 11. The complicated, essentially three-dimensional, structure of  $N_e$  distribution is clearly visible. In the same figure, the thin lines show 7 rays originating from a point on the Earth's surface at the latitude  $\lambda = 45^\circ$ . Their slopes relative to the vertical at this point are shown above the figure, positive values correspond to slope to the north, negative – to the south,  $\pm 90^\circ$  correspond to horizontals. In the coordinates  $\lambda, h$ , the rays, of course, are not straight. Integrating  $N_e$  along these lines yields STEC values. As we see, the largest contribution to the integrals is made by the heights of 200–500 km.

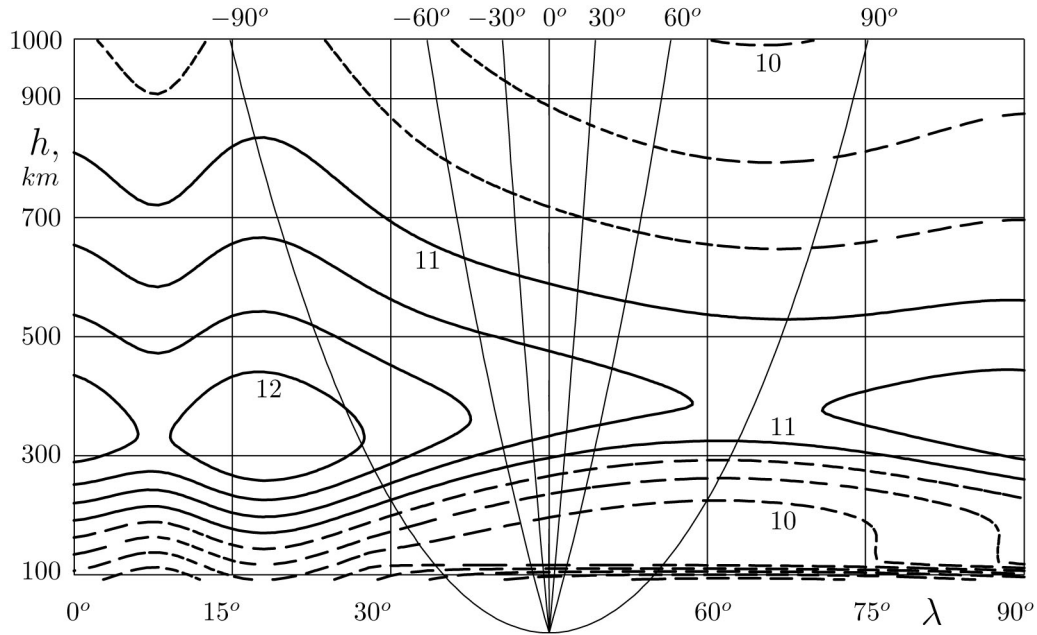


Fig. 1. Typical distribution of electron concentration in the meridional cross-section of the ionosphere

The layer between the heights 1000–2000 km and the ionosphere and plasmasphere above 2000 km add approximately 5% each. Since the nearly horizontal rays extend in the ionosphere tens of degrees of latitude away from the receiver, where the properties of the ionosphere are significantly different, simple formulae for the expression of STEC through the vertical TEC used in standard single or multi-layer models (mapping functions) can be accurate only for moderate slopes and give a significant error for other slopes.

Our interpolation framework does not prescribe closed-form explicit mapping functions; instead, we use the big data collections of STEC values from the 3D models to deduce an analogue of mapping functions (obtained as value tables, not as a formula) as we explain in the next section. In principle such tabular mapping functions could strongly depend on the position of the receiver, local time, ionospheric conditions etc. Amazingly enough we were able to obtain a universal table valid for both mid-latitude regions and (with some limitations, see Section 3.) for equatorial region, for a span of more than 15 years with small dependence on solar activity.

As the first step of our approach we need to accumulate a sufficient stock of sufficiently precise STEC values—either using real measurements (from dual-frequency receivers) or from the 3D ionospheric models described above. In this paper we choose the second option.

At the installation point of a GNSS receiver at selected times  $t_m$  a set of STEC values is

formed for azimuth angles  $a_i = 1^\circ, \dots, 360^\circ$ , and zenith angles  $z_j = 0^\circ, \dots, 90^\circ$ , both with a step  $5^\circ$  using the two empirical models of the ionosphere as two different STEC collections (they will be analysed separately). In the examples below, the time step of  $t$  equal to 1 hour was chosen, for the complete UTC 24-hour days. As test periods one day (22nd) of each month for the years 2001 (high solar activity) and 2017 (low solar activity) have been chosen. The following positions of GNSS receivers from the IGS network [2] have been chosen, with coordinates given as latitude ( $^\circ$ ), longitude ( $^\circ$ ), height (m):

1. OHI3 (Antarctica) -63.1915941 -57.5404987 32.15
2. SYOG (Antarctica) -69.002520 39.350132 50.0902
3. KERG (Kerguelen Islands) -49.210528098 70.1519885966 73.009
4. HOB2 (Hobart, Tasmania) -42.481699 147.261944 41.1
5. KAT1 (Katherine, Australia) -14.22336335 132.09117652 184.4760
6. TWTf (Taoyuan, Taiwan) 24.571296 121.095220 203.122
7. PIE1 (Pie Town, USA) 34.301506 -108.118927 2347.710900
8. AMC4 (Colorado Springs, USA) 38.803125 -104.524594 1912.489800
9. ALBH (Canada) 48.232328 -123.291464 32.0
10. KOUR (Kourou, French Guiana) 51.50792 -52.482160 25.57
11. BOR1 (Poland) 52.163704 17.042445 124.9
12. NOV1 (Novosibirsk, Russia) 55.014980 82.543416 149.98
13. SPT0 (Boras, Sweden) 57.425384 12.532884 219.9
14. SCOR (Greenland) 70.290720 -21.570121 128.5
15. THU2 (Greenland) 76.321320 -68.493000 36.1

For the stations AMC4 and PIE1 also every 22nd day of the months of 2008 and 2017 (both with low solar activity) were taken for generation of more dense STEC tables with a step  $1^\circ$  for azimuth and zenith angles and 5-minute time step.

All STEC values were computed with (nominal) precision  $10^{-6}$  TECU. NeQuick2 has internal double precision so this nominal accuracy is easy to output; for IRI-2016, which has internal single precision, we used a palliative: after forming a 3D grid of the electron density with  $2^\circ$  step along latitude,  $5^\circ$  step along longitude and 5 km step for height we convert this array to double precision and after multilinear interpolation to the slant rays (connecting a receiver and a satellite) we used the standard numeric univariate quadrature formulas to get the prescribed precision. Also some minor limitations of NeQuick2 w.r.t. solar activity upper limit were encountered; fortunately they affected only a few days in our experiments. In order to get valid results for 2017, the internal NeQuick2 table of solar activity index (provided only till 2009) was extended.

## 2. Free linear interpolation framework for STEC modeling

As explained in [10, 11], the transition from the classical univariate polynomial Lagrange interpolation basis

$$f(\hat{t}) = \sum_{n=1}^N f(t_n) \alpha_n(\hat{t}), \quad \alpha_n(\hat{t}) = \prod_{k=1, k \neq n}^N \frac{\hat{t} - t_k}{t_n - t_k} \quad (1)$$

(cf. similar formulæ for trigonometric interpolation and other fixed functional classes chosen as the bases for interpolation) to the proposed free interpolation basis is formally simple: one does not fix the explicit form of the basis functions  $\alpha_n(t)$  (we leave them “free”), instead, we

obtain the  $\alpha_n(t)$ -basis as a set of tabular functions from a large set of data: the values of the analyzed (interpolated) function  $f(t)$  at sufficiently dense set of points  $t$ , using a simple machine learning trick. Being adapted to the data under study, this  $\alpha_n(t)$ -basis gives much better results than the standard polynomial or trigonometric bases. Below we explain this new interpolation framework in detail in the form modified for the case when we have functions with three-dimensional argument: STEC values at the given receiver location depend on azimuth and zenith angles and time.

As the result of the interpolation in our framework, the value of STEC must be obtained for a ray with the direction  $(\hat{a}, \hat{z})$  defined via its azimuth and zenith angles, which we call a *target direction*. It will vary as in other interpolation approaches. First we introduce the basic concept of an *interpolation pattern*: fix  $N$  *basic directions* given by azimuths  $a_n$  and zenith angles  $z_n$ ,  $n = 1, \dots, N$ . They are chosen arbitrarily, but some rational choices will be described below. We include the target direction  $(\hat{a}, \hat{z})$  into the interpolation pattern as well. On the contrary, the time  $t$  is not included into the interpolation pattern. Once the interpolation pattern is fixed, we define the basic equation of the multidimensional linear free interpolation:

$$u(\hat{a}, \hat{z}, t_0) = \sum_{n=1}^N u(a_n, z_n, t_0) \gamma_n(\hat{a}, \hat{z}) + \varepsilon_0(\hat{a}, \hat{z}, t_0). \quad (2)$$

Now, when the form of the basic equation (2) is fixed, we proceed to the stage of finding  $\gamma_n(\hat{a}, \hat{z})$ . For this we provisionally suppose that all the STEC values (the function  $u$ ) are known — namely we take their arguments belonging to the grid of azimuth and zenith angles as well as time  $t_0$  from the large set of STEC data computed using the IRI-2016 and/or NeQuick2 model in the previous section. In particular, the basic directions and the target direction *must* be from the grid  $(a_i, z_j)$  used in the previous section. For a fixed target direction  $(\hat{a}, \hat{z})$ , and the time  $t_0$ , the interpolating basis functions  $\gamma_n(\hat{a}, \hat{z})$  are the  $N$  unknown (yet) numbers, which we call free interpolation coefficients;  $u(a_n, z_n, t_0)$  as well as  $u(\hat{a}, \hat{z}, t_0)$  are the known STEC values for the corresponding directions of the rays at this fixed moment of time  $t_0$  at the given point (receiver location) on the Earth;  $\varepsilon_0$  is the interpolation residual. We emphasize that we are trying to find time-independent functions  $\gamma_n(\hat{a}, \hat{z})$ . To find the numbers  $\gamma_n$  and the residual  $\varepsilon_0$  for the fixed  $(\hat{a}, \hat{z})$ , we shift the selected interpolation pattern (this affects only the STEC values  $u$  in all directions  $(a_n, z_n)$  and  $(\hat{a}, \hat{z})$ ) by some time step  $\Delta t$  (5 minutes or 1 hour, in our experiments). So we replace  $u(\hat{a}, \hat{z}, t_0)$  with their values for the new moment of time and obtain a similar to (2) equation with the *same coefficients*  $\gamma_n(\hat{a}, \hat{z})$  and another  $\varepsilon_0$ . Performing such time shifts  $M > N$  times, we get the system:

$$\begin{cases} u(\hat{a}, \hat{z}, t_0) = \sum_{n=1}^N u(a_n, z_n, t_0) \gamma_n(\hat{a}, \hat{z}) + \varepsilon_0(\hat{a}, \hat{z}, t_0), \\ \dots \\ u(\hat{a}, \hat{z}, t_0 + M\Delta t) = \sum_{n=1}^N u(a_n, z_n, t_0 + M\Delta t) \gamma_n(\hat{a}, \hat{z}) + \varepsilon_M(\hat{a}, \hat{z}, t_0 + M\Delta t). \end{cases} \quad (3)$$

For a fixed target direction  $(\hat{a}, \hat{z})$ , the system (3) has  $M + 1$  linear algebraic equations with  $N$  unknown numbers  $\gamma_n$  as well as  $M + 1$  numbers  $\varepsilon_m$  to be defined. We solve (3) by the standard least squares algorithm, finding  $\gamma_n$  such that  $\sum_{m=0}^M \varepsilon_m^2$  will be minimized. After reproducing these steps for all directions of the selected grid for the target directions  $(\hat{a}_i, \hat{z}_j)$  in our experiments:  $\hat{a}_i = 1^\circ, \dots, 360^\circ$ ,  $\hat{z}_j = 0^\circ, \dots, 90^\circ$  with step  $5^\circ$  (resp.  $1^\circ$ ), we get the values of  $N$  interpolating

basis functions  $\gamma_n(\hat{a}, \hat{z})$  as tables for the chosen grid of the arguments  $(\hat{a}_i, \hat{z}_j)$ . Note that in the proposed method, the interpolating functions  $\gamma_n(\hat{a}, \hat{z})$  are neither polynomials, nor trigonometric or spherical functions, etc., this explains the meaning of the term “free interpolation”.

**Secondary interpolation.** Obviously enough, in practice we need the values  $u(\hat{a}, \hat{z}, t)$  for *arbitrary* target directions  $(\hat{a}, \hat{z})$  not limited to the precomputed grid  $(a_i, z_j)$ . For sufficiently dense precomputed target grids this problem is easily solved by the standard interpolation technique (polynomial or trigonometric interpolation); this will give the values  $u(\hat{a}, \hat{z}, t)$  for any  $(\hat{a}, \hat{z})$  from the values of  $u$  computed using (2) (with omitted  $\varepsilon_0$ ) and the precomputed table of free interpolation coefficients  $\gamma_n(a_i, z_j)$  on a few grid points close to the target direction  $(\hat{a}, \hat{z})$ . Since those grid points are close to the target grid point, polynomial interpolation will give the result with high precision, not obtainable when one would try to perform a direct polynomial (or trigonometric, splines etc.) interpolation from the rarefied basis directions  $(a_n, z_n)$  of the chosen interpolation pattern; the first stage of free interpolation is essential for high precision of the result.

## 2.1. The ionospheric delay model and its use

Now we summarize the steps and procedures necessary for practical use of our free interpolation framework for high-precision computation of STEC values at a given receiver location.

First, we form the set of STEC values on a sufficiently dense grid  $(a_i, z_j)$  of directions using either NeQuick2 or IRI-2016 model. Then we fix the number  $N$  of basis directions and the directions  $(a_n, z_n)$  themselves. The larger  $N$  and the more dense the basic directions grid the higher the resulting precision of interpolation.

Second, we form the system (3) and use the least squares algorithm to find the table of free interpolation coefficients  $\gamma_n(a_i, z_j)$ . The obtained table will provide good results for a wide range of receiver locations and years of similar solar activity, as explained in the next Section, so the first and second stage shall be done *once for such locations and solar activity periods*. In fact, such tables of free interpolation coefficients can be provided to a user as ready precomputed tables in a file. One shall keep in mind that in order to get the most from the proposed interpolation framework we need the table of  $\gamma_n(a_i, z_j)$  obtained either from a large set of real measurements for dual-frequency receivers (and separating the ionospheric delays in their measurements from DCBs of the receivers and the satellites) or from the models of ionosphere and plasmasphere that incorporate higher-order effects [1, 4].

Finally, given the table of free interpolation coefficients  $\gamma_n(a_i, z_j)$  one can use the simple formula (2) (with omitted  $\varepsilon_0$ ) and secondary polynomial interpolation to compute the STEC values for arbitrary target direction, if the STEC values  $u(a_n, z_n, t)$  in the basic directions are known for the current time  $t$ . Such basic STEC values (unlike the coefficients  $\gamma_n(a_i, z_j)$ ) give the *set of parameters of our model*; they vary in time and place and shall be either provided to the user by some local or global GNSS analysis center (similar to VTEC tables provided as IGS products [2]) or found independently from local observations.

## 3. Experimental verification of the proposed method

The free interpolation framework has a lot of “hidden” freedom which can be used for further adaptation to the problems to be solved. The most important freedom is in the choice of data set used on the stage of forming the system (3).

As the first example of such a flexibility we choose only two stations from the list given in Section 1. – **AMC4** and **PIE1**, and limit the STEC data formed with NeQuick2 and IRI-2016 by the range of zenith angles  $0 \leq z \leq 60^\circ$ . This will give high-precision approximation with small number  $N$  of parameters in our model.

**Experiment 1. Stations AMC4 and PIE1, years 2008 & 2017, azimuth and zenith angle steps  $1^\circ$ ,  $0 \leq z \leq 60^\circ$ ,  $\Delta t = 5$  min.**

For each year we used interpolation patterns with  $N = 7, 10, 14, 31, 49$  points. Basic directions were chosen with increasing density for large zenith angles, so for  $N = 7$  we choose  $\{(a_n, z_n)\} = \{(0, 0), (70, 40), (190, 40), (310, 40), (10, 60), (130, 60), (250, 60)\}$ .

Let us denote the array of interpolation coefficients corresponding to some station, say **AMC4**, and some year, say 2008 and  $N = 7$  as  $\vec{\gamma}(\text{AMC4}, 2008, 7)$ . In this experiment we compute the  $\gamma$ 's only from the STEC sets obtained with NeQuick2. The vectors of residuals

$$\vec{\epsilon}(\hat{a}, \hat{z}) = \mathbf{A} \cdot \vec{\gamma}(\hat{a}, \hat{z}) - \vec{B} \quad (4)$$

(for all  $(\hat{a}, \hat{z})$  in the grid  $(a_i, z_j)$ ) are computed using the matrix  $\mathbf{A}$  and the l.h.s. vector  $\vec{B}$  of the STEC values  $u(a_n, z_n, t_m)$  and  $u(\hat{a}, \hat{z}, t_m)$  in (3). Note that we can use the array  $\gamma_m(a_i, z_j)$  in (4) for one station, say, the array  $\vec{\gamma}(\text{AMC4}, 2008, 7)$  but form  $\mathbf{A}$ ,  $\vec{B}$  from the STEC values for *another* station (and the same or another year). This is done for testing the validity of a  $\gamma$  array for several receiver locations and time. To estimate the obtained array  $\epsilon_m(a_i, z_j)$  we use the RMS estimate  $\sigma = \text{std}(\epsilon)$  averaging w.r.t. all indices  $m, i, j$ . All estimates are given in TECU.

In the following Tab. 1 in the columns 2–5 we give the  $\sigma$ 's obtained from  $\epsilon$ 's in (4) with the  $\gamma$ -array  $\vec{\gamma}(\text{AMC4}, 2008, N)$ , while in the columns 6–9 they are obtained using the  $\gamma$ -array  $\vec{\gamma}(\text{AMC4+PIE1}, 2008+2017, N)$  (the complete set of all data) with corresponding  $N$ . The columns denote the data sets used to form  $\mathbf{A}$ ,  $\vec{B}$  in (4). As one can see, already for small  $N$  we get a good approximation;  $N > 10$  are in fact unreasonable in this experiment.

Table 1. Model NeQuick2, sets  $\vec{\gamma}(\text{AMC4}, 2008, N)$ ,  $\vec{\gamma}(\text{AMC4} + \text{PIE1}, 2008 + 2017, N)$

$N$	AMC4 2008	AMC4 2017	PIE1 2008	PIE1 2017	AMC4 2008	AMC4 2017	PIE1 2008	PIE1 2017
<b>1</b>	<b>2</b>	<b>3</b>	<b>4</b>	<b>5</b>	<b>6</b>	<b>7</b>	<b>8</b>	<b>9</b>
7	0.023	0.025	0.029	0.029	0.024	0.026	0.025	0.025
10	0.016	0.018	0.020	0.021	0.017	0.018	0.018	0.018
14	0.012	0.013	0.015	0.015	0.012	0.013	0.013	0.013
31	0.006	0.007	0.007	0.008	0.006	0.007	0.006	0.006
49	0.005	0.006	0.005	0.006	0.005	0.005	0.005	0.005

In Tab. 2 we give the resulting RMS errors for  $\vec{\gamma}(\text{AMC4}, 2008, N)$  in the columns 2, 3 while in the columns 4, 5 we use  $\vec{\gamma}(\text{AMC4+PIE1}, 2008+2017, N)$  (computed with NeQuick2) substituted into (4) with  $\mathbf{A}$ ,  $\vec{B}$  formed from the the STECs of the model IRI-2016. Small RMS errors indicate universality of the  $\gamma$ -tables.

**Experiment 2. NeQuick2 data for 13 mid-latitude and 2 equatorial stations, years 2001 & 2017, azimuth and zenith angle steps  $5^\circ$ , larger zenith angles interval:  $0 \leq z \leq 80^\circ$ ,  $\Delta t = 1$  hour.**

Table 2. STECs for IRI-2016, NeQuick2-sets  $\vec{\gamma}(AMC4, 2008, N)$ ,  $\vec{\gamma}(AMC4+PIE1, 2008+2017, N)$ 

$N$	AMC4 2017	PIE1 2017	AMC4 2017	PIE1 2017
<b>1</b>	<b>2</b>	<b>3</b>	<b>4</b>	<b>5</b>
7	0.031	0.044	0.031	0.044
10	0.017	0.022	0.018	0.023

We took  $N = 19, 32$  with denser basic direction grids for  $z > 60^\circ$ . In Tab. 3. we give the respective  $\sigma$ , and used  $\gamma$ -arrays  $\vec{\gamma}(AMC4, 2001, N)$  and  $\vec{\gamma}(AMC4, 2017, N)$  for substitution into (4) for matching year and  $N$ .

Table 3. NeQuick2,  $\vec{\gamma}(AMC4, 2001, N)$ ,  $\vec{\gamma}(AMC4, 2017, N)$ 

$N$	ALBH 2001	ALBH 2017	AMC4 2001	AMC4 2017	BOR1 2001	BOR1 2017	HOB2 2001	HOB2 2017	KERG 2001	KERG 2017
19	0.036	0.057	0.029	0.050	0.046	0.060	0.052	0.081	0.041	0.069
32	0.021	0.036	0.017	0.028	0.026	0.030	0.038	0.054	0.029	0.044

$N$	KOUR 2001	KOUR 2017	NOVM 2001	NOVM 2017	OHI3 2001	OHI3 2017	PIE1 2001	PIE1 2017	SCOR 2001	SCOR 2017
19	0.039	0.056	0.043	0.062	0.062	0.087	0.036	0.051	0.048	0.075
32	0.028	0.036	0.027	0.040	0.040	0.055	0.022	0.031	0.029	0.042

$N$	SPT0 2001	SPT0 2017	SYOG 2001	SYOG 2017	THU2 2001	THU2 2017	KAT1 2001	KAT1 2017	TWTF 2001	TWTF 2017
19	0.047	0.057	0.045	0.074	0.073	0.107	0.239	0.271	0.368	0.323
32	0.027	0.031	0.028	0.045	0.041	0.055	0.119	0.152	0.183	0.159

Since the results for the equatorial stations KAT1, TWTF are much worse let us compute the  $\gamma$ -sets for those stations, separately for each year, station and  $N$ . Tab. 4 gives the obtained  $\sigma$ 's for matching years, stations and  $N$ .

Table 4. NeQuick2, matching  $\vec{\gamma}(KAT1, year, N)$ ,  $\vec{\gamma}(TWTF, year, N)$ 

$N$	KAT1 2001	KAT1 2017	TWTF 2001	TWTF 2017
19	0.283	0.269	0.225	0.468
32	0.072	0.138	0.103	0.200

Next we tried forming the  $\gamma$ -sets using the united NeQuick2 data for *all 15 stations and years*. The resulting  $\sigma$ 's for  $N = 19, 32$ , averaged over all stations separately for the years 2001, 2017 are given in the Tab. 5.

**Experiment 3. IRI-2016 data for 13 mid-latitude and 2 equatorial stations, years 2001 & 2017, azimuth and zenith angle steps  $5^\circ$ , larger zenith angles interval:  $0 \leq z \leq 80^\circ$ ,  $\Delta t = 1$  hour.**



In this experiment we use the  $\gamma$ -arrays  $\vec{\gamma}(\text{AMC4}, 2001, N)$  and  $\vec{\gamma}(\text{AMC4}, 2017, N)$  obtained using *NeQuick2*, for substitution into (4) for matching year and  $N$  and  $\mathbf{A}$ ,  $\vec{B}$  in (4) formed from the STECs of the model IRI-2016. Tab. 6 gives the obtained  $\sigma$ 's for matching years and  $N$  for each station separately. As we can see, the results in most cases approximately are twice larger than in Tab. 1, so universality of the *NeQuick2*  $\gamma$ -tables was not as good as shown in Tab. 2. PIE1 was not processed due to IRI-2016 height limitations.

Table 5. *NeQuick2*, all stations and years

$N$	All stations 2001	All stations 2017
19	0.073	0.036
32	0.029	0.017

Table 6. IRI-2016, all stations and years, *NeQuick2*  $\gamma$ -tables

$N$	ALBH 2001	ALBH 2017	AMC4 2001	AMC4 2017	BOR1 2001	BOR1 2017	HOB2 2001	HOB2 2017
19	0.096	0.033	0.001	<0.001	0.137	0.051	0.111	0.044
32	0.039	0.016	0.001	<0.001	0.078	0.041	0.064	0.029

$N$	KERG 2001	KERG 2017	KOUR 2001	KOUR 2017	NOVM 2001	NOVM 2017	OHI3 2001	OHI3 2017
19	0.084	0.045	0.089	0.025	0.140	0.056	0.182	0.060
32	0.053	0.034	0.040	0.015	0.093	0.047	0.113	0.033

$N$	SCOR 2001	SCOR 2017	SPT0 2001	SPT0 2017	SYOG 2001	SYOG 2017	THU2 2001	THU2 2017
19	0.097	0.036	0.148	0.062	0.094	0.040	0.076	0.027
32	0.046	0.027	0.118	0.053	0.050	0.025	0.032	0.015

For equatorial stations the results are again significantly worse:

$N$	KAT1 2001	KAT1 2017	TWTF 2001	TWTF 2017
19	0.302	0.166	0.800	0.154
32	0.119	0.075	0.342	0.106

Now let us use the *NeQuick2*  $\gamma$ -sets formed using the data for *all 15 stations and years* (see Experiment 2), for  $N = 19, 32$  and substitute them into (4) with  $\mathbf{A}$ ,  $\vec{B}$  from IRI-2016 data. The resulting  $\sigma$ 's averaged over all stations separately for the years 2001, 2017 are given below:

$N$	All stations 2001	All stations 2017
19	0.112	0.040
32	0.041	0.014

## 4. Conclusion and outlook

The proposed free interpolation framework has substantially lower nominal errors than many other models used in GNSS practice, still keeping the modeling algorithm very simple. Its validity for ionospheric data from real measurements (as well as feasibility of separation of receiver+satellite DCBs) will be reported in subsequent publications. A remarkable property of stability of the best fitted coefficients of our model (without adaptation to the day/night or seasonal variation of the ionosphere) should be explored in more detail, as well as weak dependence of the coefficients on solar activity.

*S. P. Tsarev was supported by the grant from the Ministry of Education and Science of the Russian Federation no. 1.8591.2017/6.7.*

## References

- [1] S. Banville, et al., On the estimation of higher-order ionospheric effects in precise point positioning, *GPS Solutions*, **21**(2017), no. 4, 1817–1828.
- [2] IGS network and products: <http://www.igs.org/network>, <http://www.igs.org/products>.
- [3] IERS Conventions (2010). Gérard Petit and Brian Luzum (eds.). (IERS Technical Note 36) Frankfurt am Main: Verlag des Bundesamts für Kartographie und Geodäsie, 2010.
- [4] M. Hernández-Pajares, J.M. Juan, J. Sanz, et al., The ionosphere: effects, GPS modeling and the benefits for space geodetic techniques, *J. of Geodesy*, **85**(2011), no. 12, 887–907.
- [5] H. Lyu, M. Hernández-Pajares, M. Nohutcu, et al., The Barcelona ionospheric mapping function (BIMF) and its application to northern mid-latitudes, *GPS Solutions*, **22**(2018), 1–13.
- [6] A.A. Mylnikova, Yu.V. Yasyukevich, V.V. Demyanov, Determination of the absolute vertical total electronic content in the ionosphere using GLONASS/GPS data, *Solar-Terrestrial Physics*, **24**(2013), 70–77 (in Russian).
- [7] D. Roma-Dollase, M. Hernández-Pajares, A. Krankowski, et al., Consistency of seven different GNSS global ionospheric mapping techniques during one solar cycle, *Journal of Geodesy*, **92**(2018), no. 6, 691–706.
- [8] S. Radicella, The NeQuick model genesis, uses and evolution, *Annals of Geophysics*, **52**(2010), no. 3-4, <https://t-ict4d.ictp.it/nequick2>
- [9] D. Bilitza, D. Altadill, V. Truhlik, V. Shubin, I. Galkin, B. Reinisch, X. Huang, International Reference Ionosphere 2016: From ionospheric climate to real-time weather predictions, *Space Weather*, **15**(2017), 418–429, <http://irimodel.org/IRI-2016/>.
- [10] A. Pustoshilov, S. Tsarev, Universal Coefficients for Precise Interpolation of GNSS Orbits from Final IGS SP3 Data, International Siberian Conference on Control and Communications, SIBCON 2017 - Proceedings, <http://ieeexplore.ieee.org/document/7998463/>.
- [11] A.S. Pustoshilov, S.P. Tsarev, High-precision interpolation of the GNSS satellites orbits by machine learning on extended SP3-data, *Advances in modern radioelectronics*, **12**(2017), 48–52 (in Russian) (<http://www.radiotec.ru/article/20294#english>).

## Многомерная свободная интерполяция в задаче высокоточного моделирования ионосферной задержки сигналов в средних широтах и вблизи экватора

**Сергей П. Царев**

Институт космических и информационных технологий  
Сибирский федеральный университет  
Свободный, 79, Красноярск, 660041  
Россия

**Валерий В. Денисенко**

Институт вычислительного моделирования СО РАН  
Академгородок, 50/44, Красноярск, 660036  
Институт математики и фундаментальной информатики  
Сибирский федеральный университет  
Свободный, 79, Красноярск, 660041  
Россия

**Марат М. Валиханов**

Институт инженерной физики и радиоэлектроники  
Сибирский федеральный университет  
Свободный, 79, Красноярск, 660041  
Россия

---

*Стандартные модели ионосферных задержек имеют точность 1–8 TECU (стандартных единиц полного электронного содержания, ПЭС). На основе метода свободной интерполяции создана новая простая модель ионосферных задержек, имеющая точность определения наклонных ПЭС  $< 0.05$  TECU относительно наклонных ПЭС, вычисленных с помощью трехмерных моделей ионосферы NeQuick2 и IRI-2016. Предложенная модель опробована для различных положений приемника в средних и низких широтах. Показана стабильность ее коэффициентов по времени и положению приемника на поверхности Земли.*

*Ключевые слова:* ионосфера, полное электронное содержание, ГЛОНАСС, GPS, интерполяция, машинное обучение.